NeuroImage: Clinical 30 (2021) 102603

Contents lists available at ScienceDirect

NeuroImage: Clinical

journal homepage: www.elsevier.com/locate/ynicl

Structural reorganization of the cerebral cortex after vestibulo-cerebellar stroke

Julian Conrad [a,b,*], Maximilian Habs [a,b], Maxine Ruehl [a,b], Rainer Boegle [a,b,c], Matthias Ertl [d], Valerie Kirsch [a,b], Ozan Eren [a], Sandra Becker-Bense [b], Thomas Stephan [a], Frank Wollenweber [e,f], Marco Duering [e,h], Marianne Dieterich [a,b,h], Peter zu Eulenburg [b,g,h]

[a] Department of Neurology, University Hospital, LMU Munich, Germany
[b] German Center for Vertigo and Balance Disorders (DSGZ), University Hospital, LMU Munich, Germany
[c] Graduate School of Systemic Neurosciences – GSN-LMU, LMU Munich, Germany
[d] Department of Psychology, University of Bern, Switzerland
[e] Institute for Stroke and Dementia Research (ISD), University Hospital, LMU Munich, Germany
[f] Department of Neurology, Helios Dr. Horst Schmidt Kliniken, Wiesbaden, Germany
[g] Institute for Neuroradiology, University Hospital, LMU Munich, Germany
[h] Munich Cluster for Systems Neurology (SyNergy), Munich, Germany

ARTICLE INFO

Keywords:
Cerebellar
Stroke
VBM
Vestibular
Neuroplasticity

ABSTRACT

Objective: Structural reorganization following cerebellar infarcts is not yet known. This study aimed to demonstrate structural volumetric changes over time in the cortical vestibular and multisensory areas (i.e., brain plasticity) after acute cerebellar infarcts with vestibular and ocular motor symptoms. Additionally, we evaluated whether structural reorganization in the patients topographically correlates with cerebello-cortical connectivity that can be observed in healthy participants.

Methods: We obtained high-resolution structural imaging in seven patients with midline cerebellar infarcts at two time points. These data were compared to structural imaging of a group of healthy age-matched controls using voxel-based morphometry (2×2 ANOVA approach). The maximum overlap of the infarcts was used as a seed region for a separate resting-state functional connectivity analysis in healthy volunteers.

Results: Volumetric changes were detected in the multisensory cortical vestibular areas around the parieto-opercular and (retro-) insular cortex. Furthermore, structural reorganization was evident in parts of the frontal, temporal, parietal, limbic, and occipital lobes and reflected functional connections between the main infarct regions in the cerebellum and the cerebral cortex in healthy individuals.

Conclusions: This study demonstrates structural reorganization in the parieto-opercular insular vestibular cortex after acute vestibulo-cerebellar infarcts. Additionally, the widely distributed structural reorganization after midline cerebellar infarcts provides additional *in vivo* evidence for the multifaceted contribution of cerebellar processing to cortical functions that extend beyond vestibular or ocular motor function.

1. Introduction

The cerebellum is not only involved in the coordination and metrics of motor function, eye movements and postural control; it is also suggested to have a role in higher order cognition, such as executive function, visual spatial processing, language, and regulation of affect (Bodranghien et al., 2016). This is supported by the strong reciprocal polysynaptic connections between the cerebral cortex and the cerebellum. Functional and structural connections of cerebellar lobules with the frontal, parietal, and limbic cortices are associated with the motor and non-motor components of cerebellar function (Buckner et al., 2011; Stoodley and Schmahmann, 2009; Strick et al., 2009).

Due to their well described anatomy, ocular motor and vestibular symptoms might be a helpful tool to evaluate cerebello-cerebral reorganization after a cerebellar infarct (Dieterich and Brandt, 2015; Kheradmand and Zee, 2011).

We investigated targeted structural reorganization on a whole-brain level following isolated cerebellar infarcts with vestibular and ocular

* Corresponding author at: Department of Neurology and German Center for Vertigo and Balance Disorders (DSGZ), Marchioninistr. 15, 81377 Munich, Germany.
E-mail address: Julian.conrad@med.uni-muenchen.de (J. Conrad).

https://doi.org/10.1016/j.nicl.2021.102603
Received 19 November 2020; Received in revised form 12 February 2021; Accepted 13 February 2021
Available online 23 February 2021

motor signs as the key symptoms using brain morphometry. We asked (i) whether these cerebellar infarcts would result in gray or white matter volume (GMV / WMV) changes in the vestibular and ocular motor representations of the cerebral cortex and, if so, (ii) whether these observed changes mimic cerebello-cortical connectivity patterns in healthy participants when using the overlap of the infarct regions as seeds for a resting-state functional connectivity (rsfcMRI) analysis. (iii) would cortical volume changes be restricted to the known cortical vestibular and ocular motor hubs or could they reflect the complex interactions of the cerebellum with the cerebral cortex.

2. Methods

2.1. Patients and controls

Patients with a first ever cerebellar ischemic infarct that presented to our tertiary referral center (University Hospital, LMU Munich, Germany) were screened between 2012 and 2019 for vestibular and ocular motor symptoms. Out of these rare conditions, we were able to recruit seven patients with a first ever cerebellar infarct with predominant ocular motor and vestibular symptoms (median age 65 years (range 33–79 years), four left-sided, five female, six right-handed). All patients underwent a detailed clinical and radiological work-up in the acute phase (M0) and after a follow-up period of six months (M6).

Inclusion criteria were as follows: Presence of ocular motor or vestibular symptoms, imaging confirmed cerebellar infarct on diffusion MRI without evidence of structural brainstem damage. Patients had to be able to complete the detailed ocular motor examination in the acute phase and after six months. Infarcts were classified as cerebellar based on the structural imaging evidence. Clinical findings that are not related to cerebellar function were considered the result of functional disconnection in the acute phase and do not reflect structural damage to the brainstem. Brainstem diffusion weighted sequences and brainstem T2 sequences were carefully examined to exclude concomitant brainstem infarcts. Patients with additional brainstem infarcts were excluded from the analysis. Also, patients with recurrent stroke, peripheral vestibular disorders, tumor, vascular malformation and severe white matter hyperintensities (Fazekas grade > 1 for periventricular and deep white matter hyperintensities) were excluded from the analysis (Fazekas et al., 1993).

The structural data was compared to a concurrently acquired data pool of 38 age-matched healthy controls (HC) using the identical neuroimaging protocols (median age: 68 years; range 51–79 y). Additionally, we obtained and analyzed resting-state functional connectivity

Table 1
Clinical and demographic data (n = 7). Symptoms are grouped as vestibulo-cerebellar and ocular motor cerebellar, other cerebellar and other signs. Note that "other" signs might result from functional disconnection of brainstem pathways in the acute phase or their attribution to cerebellar function has been challenged.

	Patients		**Controls**	
Age (median, range (y))	65 (33–79 y)		68 years (51–79 y)*	
Handedness n (%)				
Right	6 (85.7)		37 (97.3)	
Left	1 (14.3)		1 (2.7)	
Gender n (%)				
Female	5 (71.4)		19 (50.0)	
Male	2 (28.6)		19 (50.0)	
Patient data				
Infarct side n (%)				
Right	3 (42.9)			
Left	4 (57.1)			
Symptom onset to MRI (days, d)	2.3 ± 2.3 d; range 0–7 d			
Time to follow-up (days, d)	182 ±15.7 d; range 157–197 d			
	M0		**M6**	
Clinical test	**n**	**%**	**n**	**%**
Vestibulo-cerebellar and cerebellar ocular motor				
Rotational vertigo	5	71.4	1	14.3
Double vision	3	42.9	0	0.0
Lateropulsion	1	14.3	0	0.0
Falls	3	42.9	0	0.0
Pathological SVV score	4	57.1	0	0.0
Mean SVV (°, SD)	4.31 (± 4.35)		0.45 (± 0.64)	
Skew deviation	1	14.3	0	0.0
Ocular torsion	1	14.3	0	0.0
Downbeat nystagmus	3	42.9	0	0.0
Pathologic VOR (head impulse test)	0	0.0	0	0.0
Pathologic fixation suppression of VOR	2	28.6	0	0.0
Gaze evoked nystagmus	6	85.6	2	28.6
Dysmetria of saccades	4	57.1	0	0.0
Slowing of saccades	1	14.3	0	0.0
Disturbed optokinetic reflex	1	14.3	0	0.0
Saccadic smooth pursuit	7	100.0	4	57.2
Cerebellar other				
Cerebellar ataxia	3	42.9	3	42.9
Cerebellar dysarthria	2	28.6	0	0.0
Other				
Paresis	2	28.6	0	0.0
Hypaesthesia	3	42.9	0	0.0
Upbeat nystagmus	1	14.3	0	0.0
Slowing of speech	1	14.3	0	0.0
Spatial neglect	0	0.0	0	0.0
Contraversive pushing	0	0.0	0	0.0
Horner syndrome	0	0.0	0	0.0

SVV subjective visual vertical, DBN downbeating nystagmus, UBN upbeating nystagmus, VOR vestibulo-ocular reflex, SD standard deviation.
*p = 0.821, Mann-Whitney-*U* test.

using the thresholded cerebellar lesion map as a seed in a separate group of fifty healthy subjects ((age range: 20.5–32.3 years, mean age: 24.4 ± 3.7 years, 25 female) fc HC; Fig. 1A). Both control populations had no history of acute or chronic neurological disorders and were not on any permanent medication.

2.2. Clinical examination

All patients underwent a thorough neuro-orthoptic examination, including spontaneous eye position and gaze holding, eye movements such as smooth pursuit, saccades, optokinetic nystagmus, vestibulo-ocular reflex (VOR; Halmagyi head impulse test and / or Video-head impulse test (HIT)), and subjective visual vertical (SVV). Scores greater than ± 2.5° were considered pathological. The methodology of the SVV measurements has been described elsewhere (Table 1) (Baier et al., 2016).

2.3. Imaging

All participants underwent high-resolution structural MR-imaging on a 3 T MRI scanner (T1 FSPGR, 1 mm^3 isotropic, 176 slices, TR 6.63 ms, TE 3.15 ms [GE Signa Excite HD, Milwaukee, WI, USA] or T1 MPRAGE, 1 mm^3 isotropic, 192 slices, TR 2500 ms, TE 4.37 ms, Magnetom Verio or Magnetom Skyra, Siemens Healthcare, Erlangen, Germany; patients: GE n = 3, Siemens n = 4, the latter are part of the DEDEMAS study(Wollenweber et al., 2014); controls GE = 23, Siemens n = 17). All patients had their longitudinal MRIs on the same scanner.

Data quality estimation, preprocessing, and analysis were performed using the CAT12 toolbox, version 1450 (http://www.neuro.uni-jena.de/cat) within Statistical Parametric Mapping SPM12, version 7487 (https://www.fil.ion.ucl.ac.uk/spm/; Wellcome Department of Cognitive Neurology), using Matlab R2019b (Mathworks) after standard preprocessing including an 8 mm Gaussian smoothing kernel (Gaser and Dahnke, 2016). The modulated GM and WM images were used for the volumetric analysis.

The maximum overlap of the infarcts (non-flipped lesion maps, voxels that were lesioned in > 2 patients) was used as a seed for the functional connectivity analysis in 50 fc-HC. Two sessions (900 volumes each) of resting-state data were acquired in a 3 T Magnetom Prisma scanner (Siemens Healthcare, Erlangen, Germany) using a 64-channel head/neck coil with eyes open using a custom 3D-EPI sequence (TR 570 ms, TE 33 ms, 2.4 mm isotropic voxel size). A functional connectivity analysis was performed with the rsfMRI data using CONN toolbox version 19c (http://www.nitrc.org/projects/) for Matlab (version 2019a) (Whitfield-Gabrieli and Nieto-Castanon, 2012). Movement parameters, quality control time series, and scrubbing regressors were employed by the CONN Toolbox as first level covariates. For denoising, the following nuisance regressor time series were used to lessen their impact: white matter (WM) and cerebrospinal fluid (CSF) confounds were each considered with their first five principal components. Furthermore, six principal temporal components of the movement parameters (three translation and three rotation parameters) were employed. Images were denoised with a temporal band-pass filter (0.008–0.09 Hz). The seed-to-voxel results were thresholded at $p < 0.001$ *FWE* corrected (two-sided) together with 5000 permutations for non-parametric thresholding within the CONN toolbox.

To control for a potential head movement bias during image acquisition, all structural MRI images were visually inspected by two independent raters. In addition, we calculated automated, observer-independent parameters to control for head movement artifacts using MRIQC (Esteban et al., 2017).

2.4. Statistical analysis

Patient data at time point M0, M6 and data of the HC (one time point) were included in a 2 × 2 ANOVA approach with 'group' and 'time point' as factors. Total intracranial volume (TIV), age, and time to follow-up in days were used as covariates of no interest. T statistics were estimated for the contrasts M0 vs HC and M6 vs HC. The results were further analyzed using non-parametric permutation testing (*threshold-free cluster enhancement, TFCE*) as implemented in the CAT12 toolbox calculating 5000 permutations (Gaser and Dahnke, 2016). All results were corrected for multiple comparisons on the cluster level using *family wise error (FWE)* correction; results exceeding a threshold of $p < 0.05$ were considered significant. When applicable and available, the cytoarchitectonic maps of the occipital and temporal lobe, the insular gyri, and the parietal operculum were used to calculate the respective overlay of our results. The cytoarchitectonic results for each cluster were considered significant and were reported when either > 50% of the activated cluster lay within the respective probability map or >70% of the known anatomical reference area (e.g., OP2 in the parietal operculum) was activated. Results are shown with their peak t-score intensities. All results were visualized using the anatomy toolbox (https://www.fz-juelich.de/inm/inm-1/DE/Forschung/_docs/SPMAnatomyToolbox/SPMAnatomyToolbox_node.html), FSLeyes (version 0.32.00 https://zenodo.org/record/3530921#.Xqcxmi9XbOQ) and MRIcroGL by Chris Rorden (https://www.mccauslandcenter.sc.edu/mricrogl/).

2.5. Standard protocols and procedures

The study was performed in accordance with the 1964 Declaration of Helsinki (latest applicable revision Fortaleza 2013) and approved by the institutional review board of LMU Munich (no.094-10). All patients gave informed written consent to participate in the study.

2.6. Data availability

The dataset is not publicly available due to European Privacy laws and lack of consent for publication by the patients.

3. Results

3.1. Clinical

Details of demographic and clinical data are presented in Table 1. Lesion distribution is shown in Fig. 1A. An additional Figure showing the individual cerebellar lesions is available online. (Supplementary Fig. 1).

3.2. Imaging

No difference in the relevant head movement parameters were found between the patient groups at M0, M6 and the HC. We did not observe any difference in GMV or WMV when comparing M0 vs HC. GMV increases were evident at M6 compared to the HC. These included areas encompassing the rostral frontal cortex (cytoarchitectonic areas 24 and 32) and premotor areas 6d, 6 mr/mc, the dorsolateral prefrontal cortex (DLPFC, areas 44, 45) bilaterally, and motor area 4 and somatosensory areas 1–3 in the right hemisphere. Further GMV increases were located in the parieto-insular vestibular cortex (PIVC; insular / parieto-opercular multisensory areas OP1-4, Ig 1,2, TE1), inferior parietal lobule (PGp, PGa), intraparietal sulcus (IPS, hIP1-3), posterior parietal cortex (7a/p), and occipitoparietal junction hIP7 / PO1. Additional GMV increases were located in cytoarchitectonic areas FG1-4, entorhinal cortex, subiculum, hippocampus (DG, CA1) of the mesial temporal lobe extending anterior to the amygdala. Occipital GMV increases were found in the ventral visual stream in both hemispheres (hOC1, hOC2, hOC3v, hOC4v/la/lp, hOC5 (MT+) and in the dorsal visual stream in the right hemisphere (hOC3d, hOC4d). In the cerebellum we found GMV increases in lobule X (flocculus / paraflocculus), hemispheric lobules VI, VIII and Crus II (Fig. 1B). A GMV decrease was found in the left ventral posterior lateral thalamic nucleus (VPL, Fig. 2B).

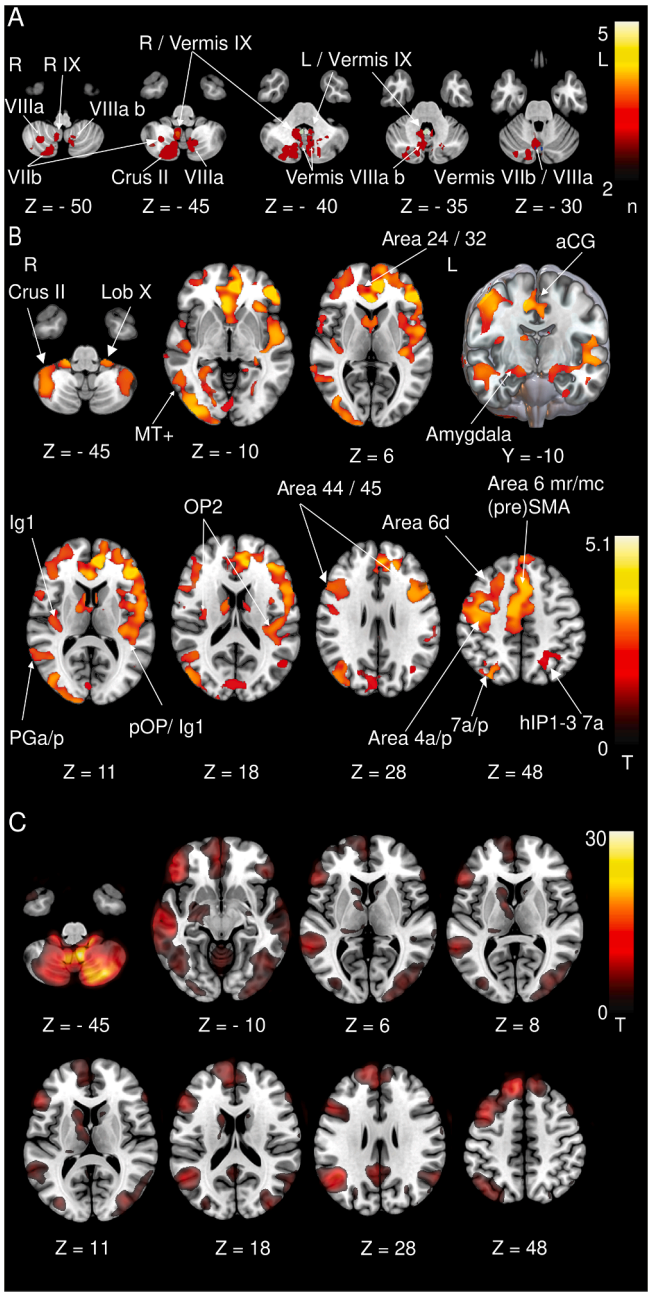

Fig. 1. **A** Thresholded cerebellar lesion map (voxels affected in > 2 patients). Infarcts were mainly located in cerebellar midline structures (vermal lobules VII, VIII, IX) but also extend into the cerebellar hemispheric lobules VII, VIII, and Crus II. Key vestibulo-cerebellar structures are overlapped with the cerebellar lesion map. Blue: ocular motor vermis, white: uvula, green: nodulus, flocculus not delineated separately as it is easily identified on imaging **B** GMV increases at follow-up (M6) compared to the control group. Increases are located in the rostral prefrontal cortex (areas 24, 32), dorsolateral and ventral prefrontal cortex (DLPFC, vPFC, areas 44, 45), (pre-) motorcortex (Area 6d, 6mr/mc, area 4a/p), anterior cingulate cortex (aCG), parieto-insular vestibular cortex (Ig 1, pOP, OP2 corresponding to PIVC), somatosensory cortex (areas 1–3), posterior parietal cortex (7a/p, hIP1-3), and along the ventral visual stream. In the cerebellum we found GMV increases in lobule X (flocculus/paraflocculus), hemispheric lobules VI, VIII (not depicted) and Crus II. **C** Resting-state functional connectivity in healthy individuals. The thresholded cerebellar lesion map was used as the seed region for this analysis. Functional connectivity with the infarcted areas was demonstrated corresponding to the GMV increases in the rostral prefrontal cortex, dorsolateral and ventrolateral prefrontal cortex (DLPFC, vPFC), the posterior parietal cortex, and along the ventral visual stream. aCG: Anterior cingulate gyrus, SMA: Supplementary motor area, hIP: Human intraparietal sulcus, MT+: Motion-sensitive middle temporal area, OP: Parietal opercular cortex, Ig: Insular granular area 1 (posterior long insular gyrus). A Voxels lesioned in > 2 patients. B, C thresholded at $p < 0.001$, *FWE* corrected. (For interpretation of the references to colour in this figure legend, the reader is referred to the web version of this article.)

WMV increases included motor areas (the corticospinal tract (CST) and the corpus callosum (CC)) and intrahemispheric association tracts. In the cerebellum WMV increases were located around lobules VIII, IX, X extending to the cerebellar hemispheric lobules VI, VIII, Crus I, II (Fig. 2A). WMV decreases were located close to temporal area MT+ and area 4 in the left hemisphere (Fig. 2B).

A direct comparison of timepoints M0 with M6 was not methodologically sound because the necessary minimal amount of permutations

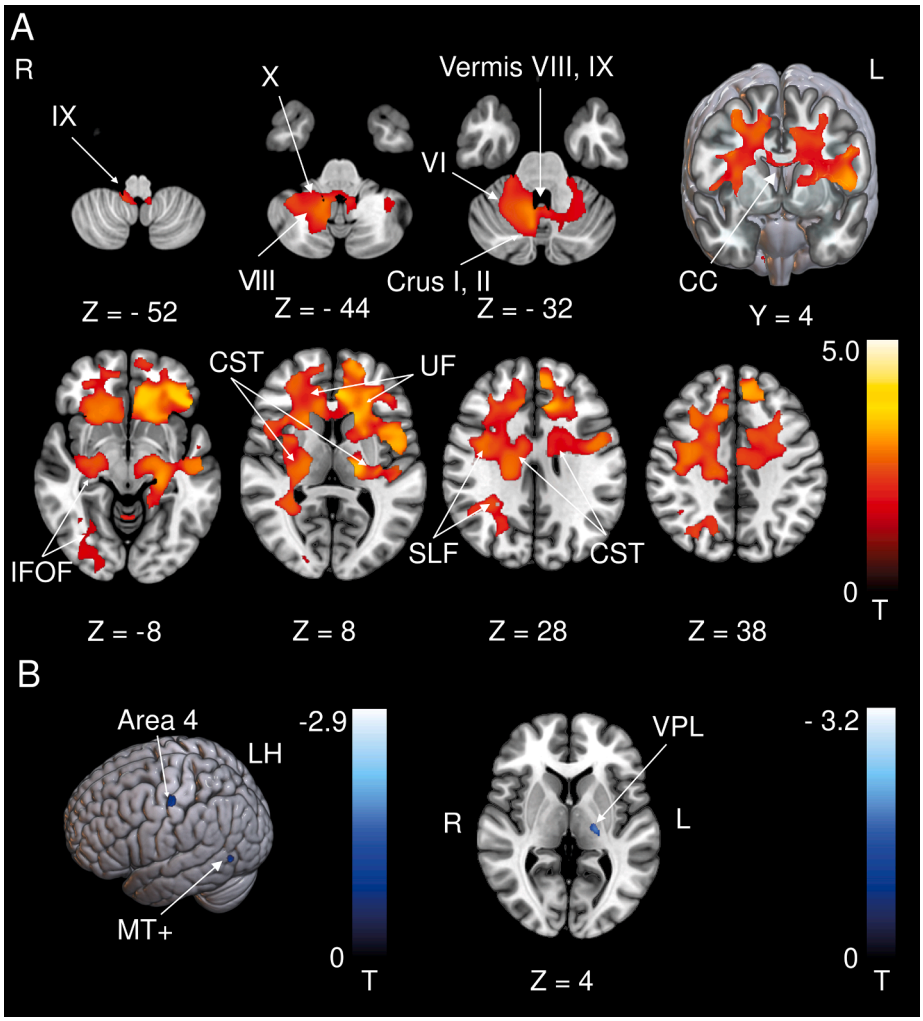

Fig. 2. A WMV increases at follow-up (M6) compared to the control group. WMV increases were located in frontal (pre-) motor areas including the corticospinal tract and the corpus and genu of the corpus callosum connecting the DLPFC and vPFC of both hemispheres. Additional WMV increases were evident in intrahemispheric association tracts (IFOF, UF, SLF). Cerebellar WMV increases were located around lobules VIII, IX, X extending to the cerebellar hemispheric lobules VI, VIII, Crus I, II. **B** GMV and WMV decreases at follow-up (M6) compared to the control group. WMV decreases were located around left cytoarchitectonic area 4 and left motion-sensitive middle temporal area (MT+). A GMV decrease was found in the ventral lateral posterior sub-nucleus of the thalamus (VPL) on the left side. CC: Corpus callosum, CST: Corticospinal tract, DLPFC: Dorsolateral prefrontal cortex, IFOF: Inferior fronto-occipital fascicle, UF: Uncinate fascicle SLF: Superior longitudinal fascicle, MT+: Motion-sensitive temporal area, vPFC: Ventrolateral prefrontal cortex, VPL: Ventral posterior lateral sub-nucleus of the thalamus. A thresholded at $p < 0.001$, *FWE* corrected for visualization, B thresholded at $p < 0.05$, *FWE* corrected.

could not be calculated.

3.3. GMV changes mirror resting-state functional connectivity in healthy controls (fc-HC group)

As for the structural changes, we found correlations of the cerebellar lesion sites with the DLPFC, the rostral frontal areas 24 and 32, the ventral visual stream including the motion sensitive middle temporal areas (MT+) and the posterior parietal cortex (Fig. 1C).

4. Discussion

In predominantly midline cerebellar infarcts, we could demonstrate widespread structural reorganization in the cerebral cortex. This structural response was very similar to functional connectivity observed in a separate cohort of healthy volunteers (fc-HC). In this group, we used the overlap image of the cerebellar infarcts as the seed region for the functional connectivity analysis. It is well-known that the vascular territories affected by ischemic infarcts as well as anatomical landmarks do not necessarily follow functional topography (Strick et al., 2009). Therefore, in the case of an ischemic infarct, multiple cerebellar lobules and functional subunits might be affected. It is our interpretation that this is reflected in the widely distributed cortical response to circumscribed cerebellar lesions and the corresponding similarities in resting state functional connectivity. Some, but not all of these changes can be attributed to reorganization within the vestibular system.

The results are in line with the established anatomical connections between the cerebellum and the frontal cortex as well as the multisensory association areas in the parietal and limbic lobes. Our findings extend our knowledge to structural reorganization following cerebellar infarcts for the first time (Bodranghien et al., 2016; Stoodley and Schmahmann, 2009). The infarct areas represent established key structures of vestibulo-cerebellar processing in primates, such as the nodulus, uvula, and flocculus (Fig. 1A) (Ruehl et al., 2017). It is therefore our interpretation that the GMV increases within the parieto-opercular insular cortex could be the direct result of cortical vestibular adaption during the recovery phase of a vestibulo-cerebellar infarct (zu Eulenburg et al., 2012). Additionally, the widely distributed neuroplastic changes across all lobes provide ample evidence for the multisensory and multi-faceted influence of the cerebellum and its connectivity gradients on the organization of the entire cerebral cortex (Guell et al., 2018).

Interestingly, volumetric increases were detected even in the cerebellum itself. While multiple cerebellar areas provide distinct vestibulocerebellar and ocular motor functions, some redundancy in terms of function is also seen in different cerebellar areas (Kheradmand and Zee, 2011). A remarkable feature of the cerebellum is the potential for rapid and thorough compensation of clinical deficits. Different mechanisms have been proposed for acute vs. chronic cerebellar injury (Mitoma et al., 2020). Therefore, one can speculate that the volumetric increases represent such a “backup” mechanism to preserve function after an ischemic infarct. Interestingly, these cerebellar volume increases included the (para-) flocculus. Floccular volume increase could be a compensatory strategy if vestibulo-cerebellar hubs in the nodulus and

uvula are lesioned. However, great caution is warranted when interpreting volumetric changes in proximity to the ischemic lesion. Therefore, our interpretation mainly focuses on the distant volumetric changes in the cerebral cortex after cerebellar infarcts.

Volume changes in the parieto-occipital region were asymmetric. The reason for this might be the asymmetric structure of the cortico-cortical vestibular network (Raiser et al., 2020). Future studies will have to investigate structural cerebello-cerebral connectivity patterns to clarify this issue. We detected volumetric decreases in the known thalamocortical sensory vestibular projection (VPL nucleus) as well as in area MT+ and area 4 in the left hemisphere. The VPL receives multisensory - including vestibular - signals that are integrated in the brainstem and modulated by the cerebellum and are conveyed to the sensory cortical areas (Barmack, 2003; Reuss et al., 2020). Therefore, degeneration of this pathway is likely a consequence of a vestibular cerebellar lesion.

MT+ is involved in visual motion, generation of smooth pursuit eye movements and has been implicated in visual attention (Kellermann et al., 2012). Also, the ocular motor vermis (OMV) as well as the MT+ region are involved in the generation and modulation of smooth pursuit eye movements (Ilg, 2008; Kheradmand and Zee, 2011). However, the amount of volumetric increases exceeded the decreases. This deserves special consideration because remote atrophy in the cerebral cortex has been demonstrated after the resection of benign cerebellar tumors (cerebello-cerebral diaschisis) (Küper and Timmann, 2013; Patay, 2015). When examining the volumetric decreases on the individual patient level, we find diverging patterns of substantial volume reduction of which our group findings represent the overlap. In our opinion, this heterogeneity in volumetric decreases on the individual level might explain the relatively little volumetric decrease that could be detected on the group level.

The study focused on vestibular and ocular motor symptoms in patients with ischemic cerebellar infarcts. Therefore, albeit tempting, we cannot provide evidence for the presence, absence or compensation of higher order cognitive deficits after cerebellar infarcts. The results of our study provide a starting point for the investigation of cognitive deficits and their restitution after ischemic cerebellar infarcts.

While the data show widespread volumetric changes in multiple cortical areas when comparing M6 with the HC, we did not report these findings in the direct comparison between M0 and M6. This is due to methodological reasons (128 permutations possible in the comparison M0 vs M6, 5000 permutations in M0 vs HC and M6 vs HC). For the sake of methodological consistency, results that did not allow extensive permutation testing were not included.

The use of different scanners is an important point to consider when evaluating our results. Specifically, patients and controls were evenly balanced over the scanners and all patients received their longitudinal MRIs on their respective baseline scanner. Furthermore, the T1-based tissue segmentations were harmonized during preprocessing via denoising and bias field correction. The data quality estimates over the entire sample showed good to very good signal homogeneity for the different tissue types. While the use of different scanners represents a potential limitation, we are confident that it did not bias our results in any way.

Despite our congruent and robust statistical findings in this cohort, one should keep the following caveat in mind: It is not possible for this study type to differentiate the rehabilitative course of the disease from the influence of confounding lifestyle changes following the infarct.

5. Conclusion

The results of the current study provide structural evidence for cortical structural reorganization following cerebellar infarcts with vestibular and ocular motor symptoms. Additionally, the widely distributed volume increases across all cerebral lobes reflect the manifold connections between cerebellar and cerebral cortex beyond vestibular processing in humans.

Funding

This work was partially funded by the support program for research and education (Foerderprogramm fuer Forschung und Lehre, FoeFo-Le^{LMU}), the German Federal Ministry of Education and Research (German Center for Vertigo and Balance Disorders-IFBLMU under the grant code BMBF EO 0901), the Vascular Dementia Research Foundation, and the German Foundation of Neurology (Deutsche Stiftung Neurologie).

Disclosures

Dr. J. Conrad reports no disclosures relevant to the manuscript.
Dr. M. Habs reports no disclosures relevant to the manuscript.
Dr. R. M. Ruehl reports no disclosures relevant to the manuscript.
Dr. R. Boegle reports no disclosures relevant to the manuscript.
Dr. M. Ertl reports no disclosures relevant to the manuscript.
Dr. V. Kirsch reports no disclosures relevant to the manuscript.
Dr. O. E. Eren reports no disclosures relevant to the manuscript.
Dr. S. Becker-Bense reports no disclosures relevant to the manuscript.
Dr. T. Stephan reports no disclosures relevant to the manuscript.
Dr. F. A. Wollenweber reports no disclosures relevant to the manuscript.
Dr. M. Duering reports no disclosures relevant to the manuscript.
Dr. M. Dieterich reports no disclosures relevant to the manuscript.
Dr. P. zu Eulenburg reports no disclosures relevant to the manuscript.

Acknowledgements

We thank Katie Goettlinger for copy-editing the manuscript.

Appendix A. Supplementary data

Supplementary data to this article can be found online at https://doi.org/10.1016/j.nicl.2021.102603.

References

Baier, B., Conrad, J., Stephan, T., Kirsch, V., Vogt, T., Wilting, J., Muller-Forell, W., Dieterich, M., 2016. Vestibular thalamus: Two distinct graviceptive pathways. Neurology 86, 134–140.
Barmack, N.H., 2003. Central vestibular system: vestibular nuclei and posterior cerebellum. Brain Res. Bull. 60, 511–541.
Bodranghien, F., Bastian, A., Casali, C., Hallett, M., Louis, E.D., Manto, M., Marien, P., Nowak, D.A., Schmahmann, J.D., Serrao, M., Steiner, K.M., Strupp, M., Tilikete, C., Timmann, D., van Dun, K., 2016. Consensus paper: revisiting the symptoms and signs of cerebellar syndrome. Cerebellum 15, 369–391.
Buckner, R.L., Krienen, F.M., Castellanos, A., Diaz, J.C., Yeo, B.T., 2011. The organization of the human cerebellum estimated by intrinsic functional connectivity. J. Neurophysiol. 106, 2322–2345.
Dieterich, M., Brandt, T., 2015. The bilateral central vestibular system: its pathways, functions, and disorders. Ann. N. Y. Acad. Sci. 1343, 10–26.
Esteban, O., Birman, D., Schaer, M., Koyejo, O.O., Poldrack, R.A., Gorgolewski, K.J., 2017. MRIQC: advancing the automatic prediction of image quality in MRI from unseen sites. PLoS ONE 12, e0184661.
Fazekas, F., Kleinert, R., Offenbacher, H., Schmidt, R., Kleinert, G., Payer, F., Radner, H., Lechner, H., 1993. Pathologic correlates of incidental MRI white matter signal hyperintensities. Neurology 43, 1683–1689.
Gaser, C., Dahnke, R., 2016. A Computational Anatomy Toolbox for the Analysis of Structural MRI Data. Human Brain Mapping 2016.
Guell, X., Schmahmann, J.D., Gabrieli, J., Ghosh, S.S., 2018. Functional gradients of the cerebellum. Elife 7.
Ilg, U.J., 2008. The role of areas MT and MST in coding of visual motion underlying the execution of smooth pursuit. Vision Res. 48, 2062–2069.
Kellermann, T., Regenbogen, C., De Vos, M., Mößnang, C., Finkelmeyer, A., Habel, U., 2012. Effective connectivity of the human cerebellum during visual attention. J. Neurosci. 32, 11453–11460.
Kheradmand, A., Zee, D.S., 2011. Cerebellum and ocular motor control. Front. Neurol. 2, 53.
Küper, M., Timmann, D., 2013. Cerebellar mutism. Brain Lang. 127, 327–333.

Mitoma, H., Buffo, A., Gelfo, F., Guell, X., Fucà, E., Kakei, S., Lee, J., Manto, M., Petrosini, L., Shaikh, A.G., Schmahmann, J.D., 2020. Consensus paper. Cerebellar reserve: from cerebellar physiology to cerebellar disorders. Cerebellum 19, 131–153.
Patay, Z., 2015. Postoperative posterior fossa syndrome: unraveling the etiology and underlying pathophysiology by using magnetic resonance imaging. Childs Nerv. Syst. 31, 1853–1858.
Raiser, T.M., Flanagin, V.L., Duering, M., van Ombergen, A., Ruehl, R.M., Zu Eulenburg, P., 2020. The human corticocortical vestibular network. Neuroimage 223, 117362.
Reuss, S., Siebrecht, E., Stier, U., Buchholz, H.G., Bausbacher, N., Schabbach, N., Kronfeld, A., Dieterich, M., Schreckenberger, M., 2020. Modeling vestibular compensation: neural plasticity upon thalamic lesion. Front. Neurol. 11, 441.
Ruehl, R.M., Hinkel, C., Bauermann, T., Eulenburg, P.Z., 2017. Delineating function and connectivity of optokinetic hubs in the cerebellum and the brainstem. Brain Struct. Funct. 222, 4163–4185.
Stoodley, C.J., Schmahmann, J.D., 2009. Functional topography in the human cerebellum: a meta-analysis of neuroimaging studies. Neuroimage 44, 489–501.
Strick, P.L., Dum, R.P., Fiez, J.A., 2009. Cerebellum and nonmotor function. Annu. Rev. Neurosci. 32, 413–434.
Whitfield-Gabrieli, S., Nieto-Castanon, A., 2012. Conn: a functional connectivity toolbox for correlated and anticorrelated brain networks. Brain Connect. 2, 125–141.
Wollenweber, F.A., Zietemann, V., Rominger, A., Opherk, C., Bayer-Karpinska, A., Gschwendtner, A., Coloma Andrews, L., Burger, K., Duering, M., Dichgans, M., 2014. The Determinants of Dementia After Stroke (DEDEMAS) Study: protocol and pilot data. Int J Stroke 9, 387–392.
zu Eulenburg, P., Caspers, S., Roski, C., Eickhoff, S.B., 2012. Meta-analytical definition and functional connectivity of the human vestibular cortex. Neuroimage 60, 162–169.